

MODELING WATER SEEPAGE INTO HEATED WASTE EMPLACEMENT DRIFTS AT YUCCA MOUNTAIN

Jens Birkholzer, Sumit Mukhopadhyay, Yvonne Tsang

Lawrence Berkeley National Laboratory
ESD, MS 90-1116, 1 Cyclotron Road
Berkeley CA 94720 USA
e-mail: jtbirkholzer@lbl.gov

ABSTRACT

This paper describes numerical prediction of the coupled thermal-hydrological processes (TH) in the vicinity of waste emplacement drifts during the heating phase of the proposed geologic repository for nuclear waste at Yucca Mountain, Nevada. Heating of rock water to above-boiling conditions induces water saturation changes and perturbed water fluxes that affect the potential of water seepage into drifts. In addition to the capillary barrier at the rock-drift interface—independent of the thermal conditions—a second barrier exists to downward percolation at above-boiling conditions. This barrier is caused by vaporization of water in the fractured rock overlying the repository. A TOUGH2 simulation model was developed to analyze the combined effect of these two barriers; it accounts for all relevant TH processes in response to heating, while incorporating the capillary barrier condition at the drift wall. Model results are presented for a variety of simulation cases.

INTRODUCTION

Predicting the amount of water that may seep into waste emplacement drifts is essential for assessing the performance of the proposed geologic nuclear waste repository at Yucca Mountain, Nevada. The repository is to be located in thick, partially saturated fractured tuff. Modeling seepage in such flow conditions involves evaluation of the capillary barrier behavior of the fractured rock at the rock-drift

interface. For ambient conditions, the amount of seepage into drifts at Yucca Mountain was assessed in a combined experimental and modeling analysis (Finsterle and Trautz et al., 2001; Ghezzehei et al., 2003). Predictive studies have also determined that heterogeneity in the flow domain is a key factor for ambient seepage at Yucca Mountain, since it causes channelized flow and local ponding (Birkholzer et al., 1999). In general, the rates of ambient seepage are related to the rock properties in the drift vicinity, the size and shape of the drift, the degree of heterogeneity, and the local percolation flux.

During the first several hundred years following waste emplacement, the fractured rock in drift vicinity will be heated to above-boiling temperatures, caused by the radioactive decay of the nuclear waste. Boiling of rock water will give rise to significant thermal and hydrological (TH) perturbation of the ambient state, with the main processes schematically illustrated in Figure 1. As the pore water in the rock matrix vaporizes, the vapor moves away from the drift through the permeable fracture network, driven primarily by the pressure increase caused by boiling. In cooler regions away from the drift, the vapor condenses in the fractures, where it can drain either toward the heat source from above or away from the drift into the zone below the heat source. With continuous heating, a hot dryout zone will develop close to the heat source. This zone is expected to extend to a maximum distance of approximately 5 to 10 m from the drift wall. Since water percolating

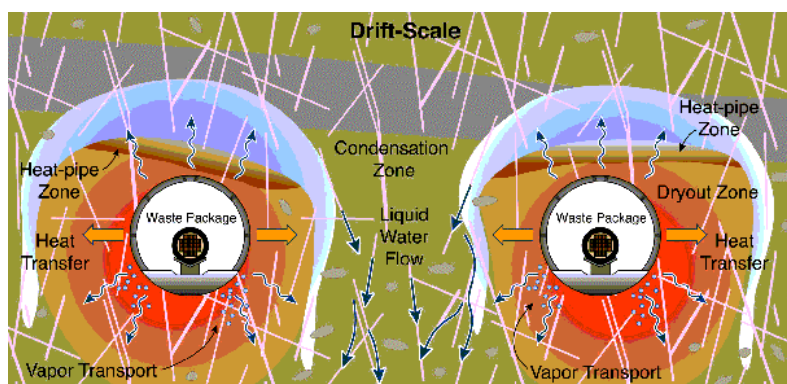


Figure 1. Schematic of expected TH processes in response to repository heating. (The drip shield above waste packages is not shown here for simplicity.)

down towards the repository will be subject to vigorous boiling, this dryout zone forms an effective vaporization barrier that limits seepage, in addition to the capillary barrier at the rock-drift interface. On the other hand, condensed water will form a zone of elevated water saturation above the rock dryout zone. Water from this zone may be mobilized to flow rapidly down towards the drift. This effect may promote seepage, particularly at later times when rock temperatures have decreased below boiling.

While in various model studies have investigated the thermal-hydrological conditions in the unsaturated “hot” environment at Yucca Mountain (e.g., Pruess et al., 1990; Buscheck et al., 2002), the magnitude and evolution of seepage at Yucca Mountain have not been explicitly addressed in these studies. Therefore, in this paper, the combined effect of vaporization and capillary barriers on “thermal seepage” (i.e., seepage during the time that flow is perturbed due to heating) is evaluated with a heterogeneous drift-scale dual-permeability process model. The conceptual framework for describing the TH conditions is based on models that accurately represent the thermal response of large *in situ* heater tests (Birkholzer and Tsang, 2000). The specific modeling framework for seepage, however, is consistent with the method employed in the ambient seepage studies cited above (Birkholzer et al., 1999; Ghezzehei et al., 2003). The key elements in this method—fracture permeability heterogeneity, weak capillary strength, and the effect of discrete fractures at the drift wall—have all been included in the thermal seepage model.

The thermal seepage model is applied to several simulation cases that cover the expected range of TH conditions at Yucca Mountain. Transient seepage rates during the period of enhanced temperatures are directly calculated from the model and compared to the respective seepage rates at ambient conditions. The model simulations cover a time period of 4,000 years after emplacement.

MODELING APPROACH

Conceptual Framework

Modeling of the TH processes in the fractured rock is conducted using the EOS4 module of TOUGH2. TOUGH2-EOS4 simulates the coupled transport of water, water vapor, air, and heat. It accounts for the movement of gaseous and liquid phases, transport of latent and sensible heat, phase transition between liquid and vapor, and vapor pressure lowering. Fractured rock is treated as a dual-permeability domain, where the fractures and the rock matrix are represented as two separate, overlapping continua (Doughty, 1999).

The seepage part of the model incorporates several conceptual elements that are important for ambient seepage (Birkholzer et al. 1999; Ghezzehei et al. 2003). A stochastic continuum model is implemented for fractures near the drift that considers the small-scale variability of permeability to account for flow channeling. Fracture permeability is represented as a stochastic field, with spatial variability estimated from small-scale air-permeability testing. Another key element of the model is a comparably small capillary-strength parameter close to the drift wall, derived from inverse modeling of niche liquid-release tests (Ghezzehei et al., 2003). Finally, a specific seepage boundary condition is implemented at the rock-drift interface. The circular-shaped drift is represented as an open cavity with a zero capillary-strength parameter. While not explicitly simulated, the effect of small-scale wall roughness and/or small fractures cutting into the opening is accounted for by setting the length of the last vertical connection between the drift interface and the adjacent gridblock representing the fracture continuum to 0.05 m. The choice of this distance affects seepage because no horizontal flow can occur within 0.05 m of the wall. Seepage from the rock matrix into the drift is unlikely because of the strong capillarity and low permeability of the matrix; thus, seepage from the matrix is not considered in the thermal seepage model. In this model, water that seeps into the drift is collected without further consideration of the flow processes that may occur within the open cavity. (Modeling of in-drift flow processes is not relevant for the scope of this study.

Model Domain and Boundary Conditions

The TH behavior of the fractured rock is simulated in a two-dimensional (2-D) vertical model domain perpendicular to the drift axis. (A fully three-dimensional (3-D) simulation of drift-scale coupled processes is not feasible because of computational limitations.) The TH simulation requires a large vertical model domain because the thermally disturbed zone extends far into the overlying and underlying geological units. Also, with the focus on near-drift conditions, it is important to represent the drift vicinity with refined discretization. The main deviations between a 3-D and a 2-D model occur at the end of each emplacement drift and at the edges of the repository. Such effects—and those additional effects stemming from heat output variation and emplacement-time differences between individual waste packages—are accounted for by considering several sensitivity cases for the thermal load. Also note that, with respect to the effectiveness of the capillary barrier for seepage into drifts, a 2-D representation is more critical in most cases of heterogeneous fracture permeability fields because the potential diversion of flow in the third dimension is neglected.

In the vertical direction, the ground surface of Yucca Mountain is taken as the top model boundary. The water table below the repository is used as the bottom boundary. To increase the computational efficiency of the simulation runs, we apply symmetry assumptions for reduction of the model domain in the lateral direction, perpendicular to the drift axis. The current repository design of parallel drifts spaced at 81 m can be represented as a series of symmetrical, identical half-drift models with vertical no-flow boundaries between them. Thus, the numerical mesh can be reduced to a half-drift model with a width of 40.5 m, extending from the drift center to the midpoint between drifts (see close-up view of repository units in Figure 2). Different cross sections (submodels) are studied, depending on the location of the repository drifts. For example, the cross section depicted in Figure 2 has the emplacement drift located in the Topopah Spring Tuff middle nonlithophysal unit (Tptpmn).

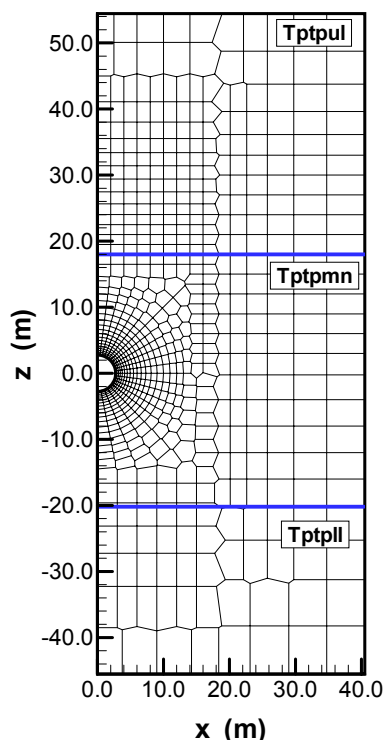


Figure 2. Close-up view of discretization of drift vicinity in the thermal seepage model.

Both the top and bottom boundaries are treated as Dirichlet-type conditions with specified constant temperature, gas pressure, and liquid saturation values. The ground surface of the mountain at the top of the model domain is represented as an open atmosphere. The water table at the bottom of the model domain is represented as a flat, stable surface. Surface infiltration, as discussed below, is applied using a source term for the first rock gridblocks at the

top boundary. The thermal load of the waste packages is placed into the appropriate model elements in the open drift. An average linear thermal load is assumed that decreases with time as a result of the radioactive decay. All lateral boundaries are no-flow boundaries for water, gas, and heat.

Simulation Cases

Many different simulation runs with different parameter values are performed to cover the expected range of uncertainty and variability in these parameters. Parameters that are varied are those expected to impact seepage during the thermal period—e.g., thermal-operating mode and percolation flux. Temperature conditions, for example, are expected to vary considerably in the repository, arising from heat output variation among individual waste packages, emplacement-time differences among repository sections, and three-dimensional (3-D) edge effects. Therefore, three different thermal operating modes are analyzed in this study. “Reference mode” denotes a thermal load representative of the average thermal conditions for the current repository design, resulting in maximum rock temperatures above the boiling point of water for several hundred years close to the emplacement drifts. The other thermal-operating modes are studied as sensitivity cases, resulting in rock temperature conditions that can be as high as 140°C (for the so-called “high-temp” mode) or that will barely exceed boiling temperature (for the so-called “low-temp mode”).

Surface infiltration at Yucca Mountain is also expected to vary significantly in space, and it will be affected by future climate changes. In this study, three climate periods are assumed, with average infiltration values of 6 mm/yr for the present-day climate (up to 600 years from now), 16 mm/yr for the monsoon climate (600–2,000 years from now), and 25 mm/yr for the glacial transition climate (more than 2,000 years from now). Within the unsaturated zone, downward flow is mostly defined by the amount and spatial variability of surface infiltration. However, there may be additional flux variation as a result of heterogeneity in rock properties, flow diversion, and flow focusing. The boundary flow values imposed at the top of the thermal seepage model must accommodate these additional effects to cover the resulting range of percolation fluxes within the repository units. This is achieved by multiplying the average infiltration rates by factors of five, ten, and 20, giving percolation values of 125, 250, and 500 mm/yr, respectively, for the glacial transition climate. For convenience, the above factors of 5, 10, and 20 are referred to hereafter as flow focusing factors, though these factors also account for flow uncertainty and variability.

Note that rock properties relevant for thermal seepage have also been varied in a sensitivity study not presented in this paper. These rock properties for thermal seepage are the permeability, the capillary-strength parameter, and the thermal conductivity of the fractured rock in the drift vicinity. The first two parameters significantly affect the diversion capacity of the fractured medium at the rock-drift interface. The last parameter is important for the thermal conditions in the drift vicinity. All other parameters, and all parameters in those geologic units away from the repository drifts, remain unchanged, with their values defined from mountain-scale calibration.

MODEL RESULTS

For the reference thermal mode, the heat generated from the waste canisters results in maximum rock temperatures at the drift wall between 120°C and 130°C, depending on the amount of percolation considered (see Figure 3). For the simulation run without flow focusing, the period of above-boiling rock temperature is about 1,000 years. Increasing the percolation flux has considerable impact on the temperature evolution. Elevated infiltration as a result of flow focusing leads to cooler temperatures and a shorter boiling period. Strong heat-pipe signals (with temperatures remaining at boiling) become particularly evident for flow focusing factor 20, where the infiltration fluxes imposed at the top model boundary are 120, 320, and 500 mm/yr, respectively, for the three climate periods.

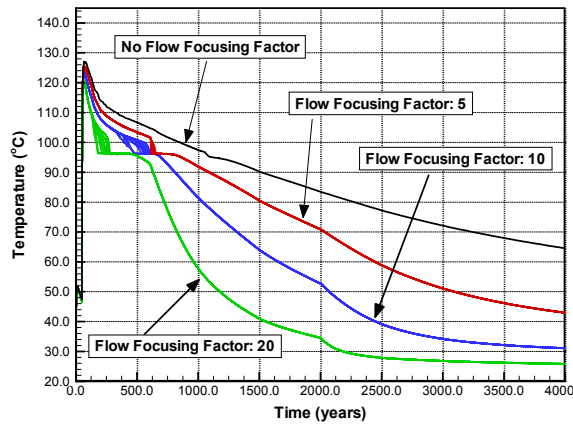
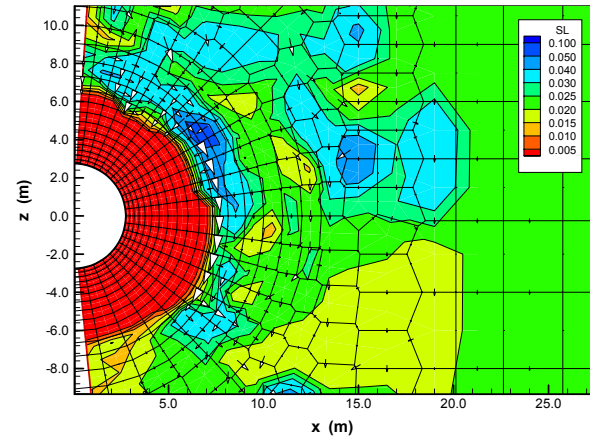


Figure 3. Rock temperature at the drift wall for different flow-Focusing factors and reference mode thermal load.

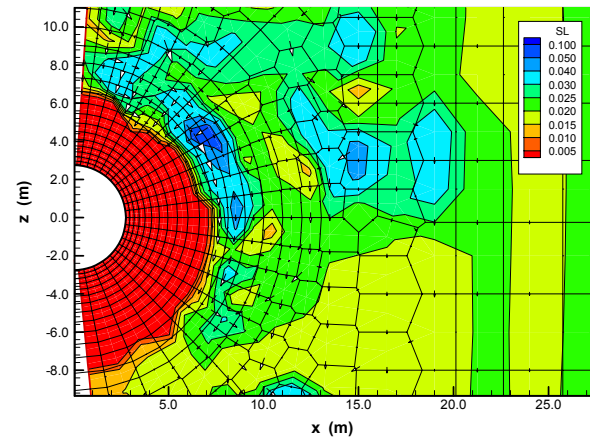
Thermally induced movement of water and gas occurs primarily in the fractures. As rock water in the matrix boils off, vapor is driven into the fractures and away from the boiling zone. Condensation causing water saturation to build up may lead to elevated water fluxes in the fractures. The fracture saturation contours and flux vectors in Figure 4 illustrate this

behavior. Example results are presented for the reference thermal mode and a simulation run without flow focusing. Note that three realizations of stochastic permeability fields have been simulated in this study; one is chosen in Figure 4.

100 years



500 years



1,000 years

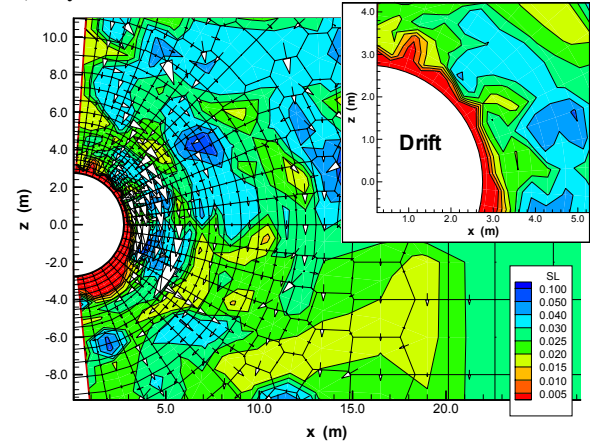


Figure 4. Fracture saturation and liquid flux vectors for reference thermal load

The fracture saturations show a dryout zone extending about 5 m above the drift crown at 100

years after emplacement. Water that percolates downward is mostly diverted around this dryout zone, effectively removing water from the drift vicinity. Outside of the dryout zone, water saturation builds up as a result of condensation. Although this saturation buildup involves only changes of a few percent on average, it is enough to increase water fluxes considerably from the ambient downward flow (the magnitude of undisturbed downward flow corresponds to the small vertical flux vectors far away from the drift). Heterogeneity of permeability gives rise to significant variation in fracture saturation and water flux. However, the effect of flow channeling is not strong enough to allow significant penetration of water into the dryout zone. It appears that the vaporization barrier is fully effective as long as rock temperature is above boiling, despite the permeability variation. At 500 years, similar flow processes occur, but the magnitude is smaller. The strongest flux perturbation occurs at early heating stages when the thermal load is intense.

At 1,000 years, the flow regime is in a transition state from a thermally perturbed system to an ambient system. The dryout zone has receded to a very small region around the drifts, and no saturation buildup is visible outside of this region. At even later times, the fractures close to the drift wall start rewetting. Whether seepage occurs for “wet” conditions at the drift wall depends on the capillary barrier capability at the rock-drift interface.

The following figures demonstrate the combined effectiveness of the vaporization barrier and the capillary barrier during the thermally perturbed time period. Only such simulation cases are presented that are likely to have seepage conditions (i.e., high percolation fluxes). In general, seepage is possible only when (a) water arrives at the drift wall, depending on the vaporization impact, and (b) the saturation at the drift wall exceeds a given threshold value, defined by the zero capillary condition in the drift and the 0.05 m vertical connection. Figure 5 shows the evolution of fracture saturation at all grid blocks adjacent to the drift wall for a simulation case with a flow focusing factor of 10. The saturation curves in Figure 5 demonstrate that no water arrives at the drift during the boiling period. As rock temperature decreases and the first stepwise change in infiltration occurs at 600 years, the saturation values build up strongly, while significant variability in saturation becomes evident.

The evolution of seepage into drifts for this case is given in Figure 6. The magnitude of seepage is provided in percent, relative to the total liquid flux percolating with constant top boundary flow rate through an area corresponding to the footprint of the drift. The transient curve of thermal seepage is to be

compared with the ambient seepage percentage, which is also depicted in Figure 6. Ambient seepage was evaluated by running the thermal seepage model without thermal load until a steady state was achieved, separately for each climate period. As a result of the saturation increases, seepage starts to occur at about 1,400 years after waste emplacement, while still in the monsoon climate period (Figure 6). With the stepwise increase of infiltration at 2,000 years, the seepage percentage increases considerably, and water starts to seep at a second location along the drift wall. At the end of the simulation period, the thermal seepage percentage is at 17%, slightly smaller than the long-term ambient value of 20% for a 250 mm/yr percolation flux. Apparently, the flow system at 4,000 years is still adjusting to the infiltration change at 2,000 years; a steady-state situation has not been reached.

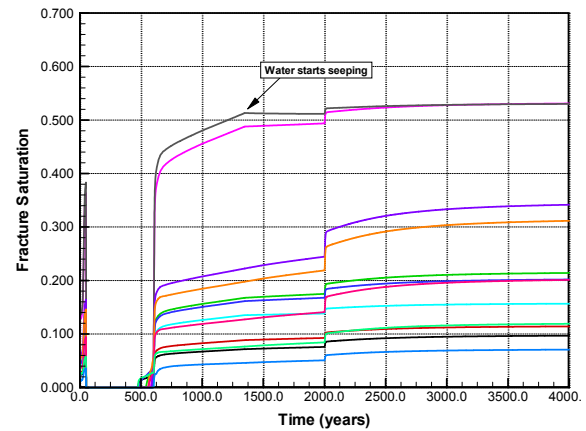


Figure 5. Fracture saturation along the drift periphery for reference thermal mode and flow focusing factor 10

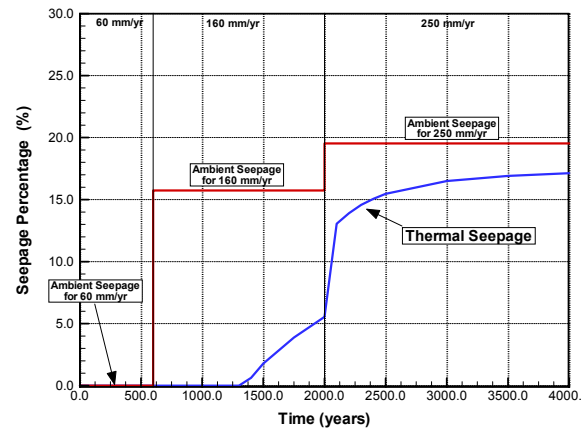


Figure 6. Seepage percentage for reference thermal mode and flow focusing factor 10

Note that the long-term ambient seepage from steady-state simulation runs performed with the present-day infiltration rate—i.e., 60 mm/yr—is zero. In other

words, even without heating of the repository, the capillary barrier at the drift wall is predicted to be fully effective during the first 600 years after waste emplacement. That no water arrives at the drift wall during these first 600 years as a result of the vaporization barrier provides additional confidence, as two fully effective barriers operate simultaneously and independently.

The following figures show the evolution of thermal seepage for other simulation cases. Figure 7 presents results for the second realization of the random permeability field. Figure 8 demonstrates the effect of different thermal loads. Finally, Figures 9 and 10 give results for flow focusing factors of 5 and 20, respectively.

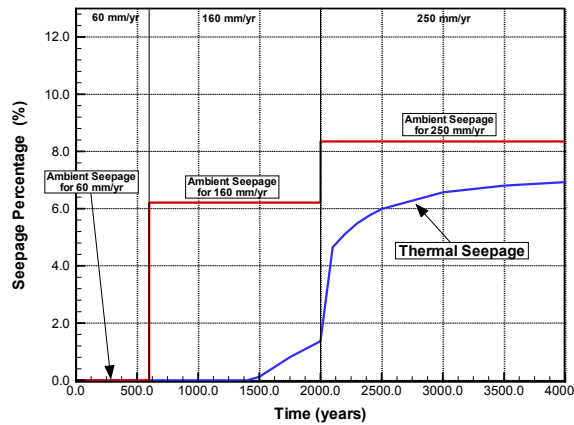


Figure 7. Seepage percentage for reference thermal mode and flow focusing factor 10 (realization 2)

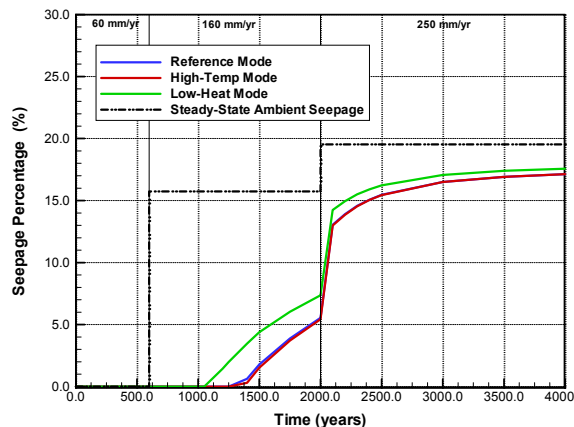


Figure 8. Seepage percentage for different thermal modes and flow focusing factor 10

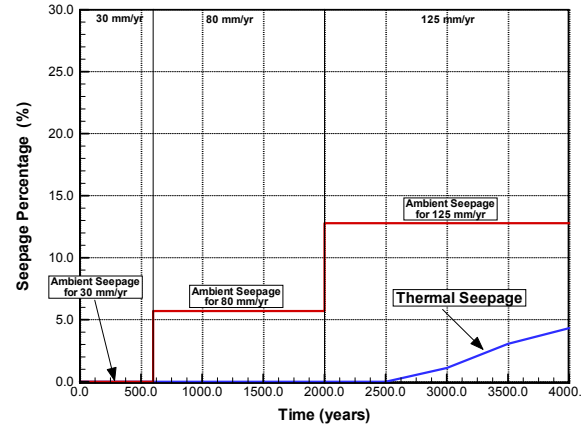


Figure 9. Seepage percentage for reference thermal mode and flow focusing factor 5

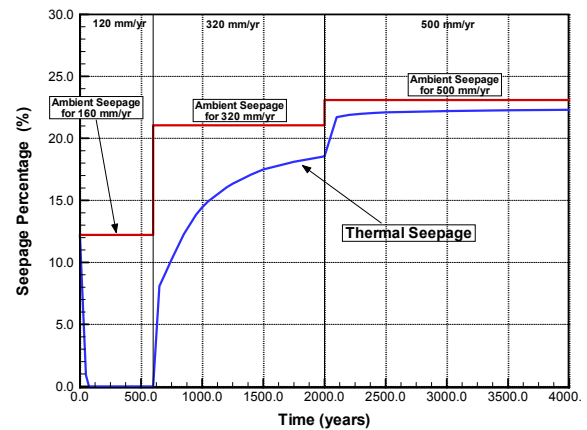


Figure 10. Seepage percentage for reference thermal mode and flow focusing factor 20

Figures 7 through 10 show considerable differences with respect to the magnitude and the evolution of thermal seepage. For example, the magnitude of seepage is much smaller in Figure 7 compared to Figure 6, a difference that can be attributed entirely to study of a different random permeability field. In Figure 8, thermal seepage for the low-temp mode starts several hundred years earlier than in the other cases, as a result of less effective vaporization of water, whereas the reference mode and the high-temp mode give almost identical results with respect to thermal seepage. This is because the temperature difference between the two latter thermal-load cases has almost vanished at the time when thermal seepage first occurs. Figures 9 and 10 demonstrate the importance of the overall percolation flux in the model domain. Thermal seepage starts much later and is smaller in magnitude for the flow focusing factor 5 case compared to the factor-20 case.

Despite the differences observed above, there are a few important observations common to all simulation cases that were studied:

- The vaporization barrier is effective as long as boiling conditions persist in the rock close to the drifts, even for high infiltration fluxes. Channelized fast flow cannot penetrate far into the superheated rock during the “hot” time period.
- Thermal seepage is always smaller than the long-term ambient seepage percentage calculated from steady-state simulation runs using the respective infiltration rate of the three climate periods.
- Whether thermal seepage occurs after the vaporization barrier has vanished depends on the effectiveness of the capillary barrier, as evaluated by the long-term ambient seepage simulations for the steady state.

SUMMARY AND CONCLUSION

A TOUGH2 simulation model was developed to evaluate the potential for seepage into drifts during the time that TH conditions are perturbed as a result of repository heating at Yucca Mountain. This model is applied to various simulation cases to cover the expected range of uncertainty and variability in seepage-relevant parameters. Transient seepage rates into the drift are directly calculated from the model.

Results demonstrate that the thermal perturbation of the flow field—giving rise to increased downward flux from the condensation zone towards the drifts—is strongest during the first few hundred years after emplacement, corresponding to the period when rock temperature is highest and the vaporization barrier is most effective. Even for high percolation fluxes into the model domain, and strong flow channeling as a result of fracture heterogeneity, water cannot penetrate far into the superheated rock during the time that rock temperature is above boiling, and model results show no seepage.

At the time when temperature has returned to below-boiling conditions and fractures start rewetting at the drift, the capillary barrier at the drift wall continues to reduce (or prevent) water seepage into the drift. Seepage is predicted to occur for such simulation cases that feature strongly heterogeneous fracture permeability fields, weak fracture capillary strength in the drift vicinity, and high percolation fluxes. In these cases, water starts to seep several hundred to a few thousand years after rock temperature has returned to below boiling, the delay caused by the slow saturation buildup in fractures. Seepage amounts increase with time, and asymptotically approach seepage rates estimated for long-term ambient conditions.

ACKNOWLEDGMENT

This work was supported by the Director, Office of Civilian Radioactive Waste Management, U.S. Department of Energy, through Memorandum Purchase Order EA9013MC5X between Bechtel SAIC Company, LLC, and the Ernest Orlando Lawrence Berkeley National Laboratory (Berkeley Lab). The support is provided to Berkeley Lab through the U.S. Department of Energy Contract No. DE-AC03-76SF00098. Review and comments of Dan Hawkes and Robin Datta from Berkeley Lab are gratefully appreciated.

REFERENCES

- Birkholzer, J., G. Li., C.-F. Tsang, and Y.W. Tsang, Modeling studies and analysis of seepage into drifts at Yucca Mountain, *Journal of Contaminant Hydrology*, 38(1-3), 349-384, 1999.
- Birkholzer, J.T., Y.W. Tsang, Modeling the thermal-hydrologic processes in a large-scale underground heater test in partially saturated fractured tuff, *Water Resources Research*, 36(6), 1431-1447, 2000.
- Buscheck, T.A., N.D. Rosenberg, J. Gansemer, Y. Sun, Thermohydrologic behavior at an underground nuclear waste repository, *Water Resources Research*, 38(3), 1-19, 2002.
- Doughty, C., Investigation of conceptual and numerical approaches for evaluating moisture, gas, chemical, and heat transport in fractured unsaturated rock, *Journal of Contaminant Hydrology*, 38(1-3), 69-106, 1999.
- Finsterle, S., R.C. Trautz, Numerical modeling of seepage into underground openings, *Mining Engineering*, 52-56, 2001.
- Ghezzehei, T., S. Finsterle, R. C. Trautz, Evaluating the effectiveness of liquid diversion around an underground opening when evaporation is non-negligible, Proceedings: TOUGH Symposium 2003, Berkeley, Calif., May 12-14, 2003.
- Pruess, K., J.S.Y. Wang, Y.W. Tsang., On thermo-hydrologic conditions near high-level nuclear wastes emplaced in partially saturated fractured tuff, 2. effective continuum approximation, *Water Resources Research*, 26(6), 1249-1261, 1990.